ACCOUNTS of chemical research

pubs.acs.org/accounts Article

Enabling Nucleophilic Reactivity in High-Spin Fe(II) Imido Complexes: From Elementary Steps to Cooperative Catalysis

Yafei Gao* and Jeremy M. Smith*

Cite This: *Acc. Chem. Res.* 2023, 56, 3392−3403 Read Online

ACCESS | Metrics & More | Article Recommendations

CONSPECTUS: Transition metal complexes featuring an M═NR bond have received great attention as critical intermediates in the synthesis of nitrogen-containing compounds. In general, the properties of the imido ligand in these complexes are dependent on the nature of the metal center. Thus, the imido ligand tends to be nucleophilic in early transition metal complexes and electrophilic in late transition metal complexes. Nonetheless, the supporting ligand can have a dramatic effect on its reactivity. For example, there are sporadic examples of nucleophilic late transition metal imido complexes, often based on strongly donating supporting ligands. Building on these earlier works, in this Article, we show that the imido ligand in a low-coordinate high-spin bis(carbene)borate Fe(II) complex is able to access previously unknown reaction pathways, ultimately leading to new catalytic transformations. We first focus on the synthesis, characterization, and stoichiometric reactivity of a highly nucleophilic Fe(II) imido complex. The entry point for this system is the intermediate-spin three-coordinate Fe(III) imido complex, which is generated from the reaction of an Fe(I) synthon with an organic azide. Alkali metal reduction leads to a series of M^+ (M = Li, Na, K) coordinated and charge-separated (M = K(18-C-6)) high-spin Fe(II) imido complexes, all of which have been isolated and fully characterized. Combined with the electronic structure calculations, these results reveal that the alkali ions moderately polarize the Fe═N bond according to $K^+ \approx Na^+ < Li^+$. As a result, the basicity of the imido ligand increases from the charged separated complex to K^+, Na^+, and Li^+ coordinated complexes, as validated by intermolecular proton transfer equilibria. The impact of the counterion on imido ligand reactivity is demonstrated through protonation, alkylation, and hydrogen atom abstraction reactions. The counterion also directs the outcome of [2 + 2] reactions with benzophenone, where alkali coordination facilitates double bond metathesis. Building from here, we describe how the unusual nucleophilicity of the high-spin Fe(II) imido complex revealed in stoichiometric reactions can be extended to new catalytic transformations. For example, a [2 + 2] cycloaddition reaction serves as the basis for the catalytic guanylation of carbodiimides under mild conditions. More interestingly, this complex also exhibits the first ene-like reactivity of an M═NR bond in reactions with alkynes, nitriles, and alkenes. These transformations form the basis of catalytic alkyne and nitrile α-deuteration and pK_a-dictated alkene transposition reactions, respectively. Mechanistic studies reveal the critical role of metal−ligand cooperativity in facilitating these catalytic transformations and suggest the new avenues for transition metal imido complexes in catalysis that extend beyond classical nitrene transfer chemistry.

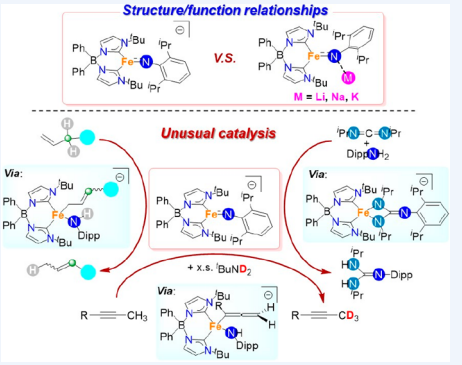

KEY REFERENCES

- Gao, Y.; Carta, V.; Pink, M.; Smith, J. M. Catalytic Carbodiimide Guanylation by a Nucleophilic, High Spin Iron(II) Imido Complex. *J. Am. Chem. Soc.* **2021**, *143*, 5324−5329.[1] This study reports the first example of a catalytic transformation that builds on stoichiometric [2 + 2] cycloaddition reactions of a late transition metal imido complex.
- Gao, Y.; Pink, M.; Smith, J. M. Alkali Metal Ions Dictate the Structure and Reactivity of an Iron(II) Imido Complex. *J. Am. Chem. Soc.* **2022**, *144*, 1786−1794.[2] The impact of the alkali metal ion on the properties of the imido ligand in a synthesis of a series of alkali metal-coordinated Fe(II) imido complexes is reported.
- Gao, Y.; Pink, M.; Carta, V.; Smith, J. M. Ene Reactivity of an Fe═NR Bond Enables the Catalytic α-Deuteration of Nitriles and Alkynes. *J. Am. Chem. Soc.* **2022**, *144*, 17165−17172.[3] The first example of ene-like reactivity involving a transition metal imido complex provides the basis for the catalytic α-deuteration of nitriles and alkynes.

Received: August 23, 2023
Revised: October 23, 2023
Accepted: October 25, 2023
Published: November 13, 2023

https://doi.org/10.1021/acs.accounts.3c00511
Acc. Chem. Res. 2023, 56, 3392−3403

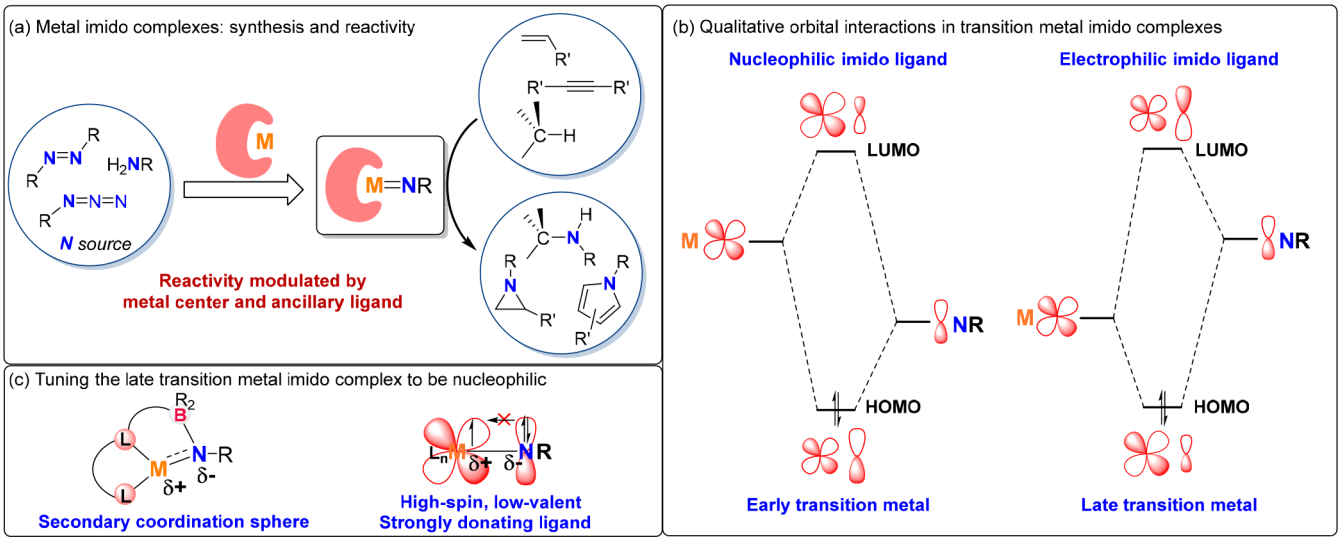

Figure 1. (a) Synthesis and reactivity of transition metal imido complexes; (b) qualitative orbital interactions in transition metal imido complexes; (c) strategies for creating nucleophilic late transition metal imido complexes.

- Gao, Y.; Li, X.; Stevens, J. E.; Tang, H.; Smith, J. M. Catalytic 1,3-Proton Transfer in Alkenes Enabled by Fe═NR Bond Cooperativity: A Strategy for pK_a-Dictated Regioselective Transposition of C═C Double Bonds *J. Am. Chem. Soc.* **2023**, *145*, 11978−11987.[4] This study demonstrates that the cooperative action of the iron-imido bond facilitates catalytic alkene transposition, with pK_a-dictated substrate selectivity.

1. INTRODUCTION

Transition metal catalysis is one of the most powerful approaches for constructing the complex organic molecules that are widely used in the pharmaceutical, agrochemical, and functional materials fields.[5−9] Significant research efforts have been made toward understanding intermediates in the catalytic cycle since their reactivity often plays a vital role in the efficiency and selectivity of the overall transformation.[10−12] While historically noble metal catalysts have received the most attention, more recently the pursuit of economical and environmentally benign catalysts has resulted in significant efforts in the development of 3d metal species.[13−15]

Since the first reports of transient transition metal−nitrogen double bonded species (M═NR),[16] research efforts have mainly focused on developing iron imido complexes in nitrene transfer catalysis.[17−19] This focus stems in part from the potential utility of the iron−nitrogen multiple bond in the efficient synthesis of nitrogen-containing compounds (Figure 1a). These species are also expected to be relevant to the development of bioinspired N_2 activation chemistry.[20] A number of routes to access imido ligands have been developed, with azides, azo compounds, and amines commonly serving as the nitrogen source.[21]

An important feature of imido complexes is that the properties of the imido ligand can be dramatically modified by the nature of the metal center (Figure 1b). Since the relevant metal-based orbitals of early transition metals are higher in energy, the imido ligand in these complexes is typically nucleophilic. A signature reaction of these complexes is the [2 + 2] cycloaddition, which is observed for a range of unsaturated substrates and forms the basis of many useful catalytic transformations.[21] On the other hand, the metal-imido bond in late transition metal congeners is more covalent, and the nitrogen atom is usually electrophilic. Catalytic transformations involving such complexes are generally restricted to nitrene transfer.[22,23]

While the metal has a strong influence on the imido ligand properties, these preferences can be overridden by the ancillary ligands. For example, Chu and co-workers have shown that a second coordination sphere borane functionality polarizes a Ni═NR bond, resulting in an imido ligand that has similar properties to those of early transition metal centers (Figure 1c).[24] Imbuing imido ligands in late transition metal centers with greater nucleophilic character may lead to catalysts that have greater substrate scope than oxophilic early transition metal complexes, e.g., in [2 + 2] reactions. More broadly, changing the fundamental properties of the imido ligand may unlock reactivity that extends beyond typical N-group transfer catalysis, leading to unprecedented reaction patterns. However, only a few strategies for achieving this are known.

While there are now many examples of iron imidos, three-coordinate complexes appear to provide a good balance between isolability and reactivity. The supporting ligand in these complexes is typically a weak-field donor, such as *β*-diketiminates and bis(pyrrolyl)methanes.[25−32] In light of our experience with strongly donating tris(carbene)borate ligands,[33−41] we were interested in extending iron imido chemistry to the stronger field bis(carbene)borate platform. Here, it is worth noting that Deng and co-workers have shown that Fe(II)/Co(II) imido complexes supported by a strongly donating *N*-heterocyclic carbene ligand display unusual nucleophilic character in reactions with a range of substrates, albeit in stoichiometric transformations.[42−44]

In this Article, we summarize the chemistry of bis(carbene)-borate iron imido complexes, with an emphasis on nucleophilic high-spin Fe(II) imido complexes. Due to the high spin state, these complexes have attenuated p → d donation from the imido ligand to the (partially) filled d orbitals of the electron rich metal center. Combined with the negative charge on the complex, this creates a nucleophilic complex (Figure 1c) in which the imido nitrogen atom is the locus of nucleophilic reactivity.

Our studies reveal that the strongly donating bis(carbene)-borate ligand stabilizes iron imido complexes with unusual

https://doi.org/10.1021/acs.accounts.3c00511
Acc. Chem. Res. 2023, 56, 3392−3403

Scheme 1. Synthesis of Fe Imido Complexes with a Bulky Bis(carbene)borate Ligand

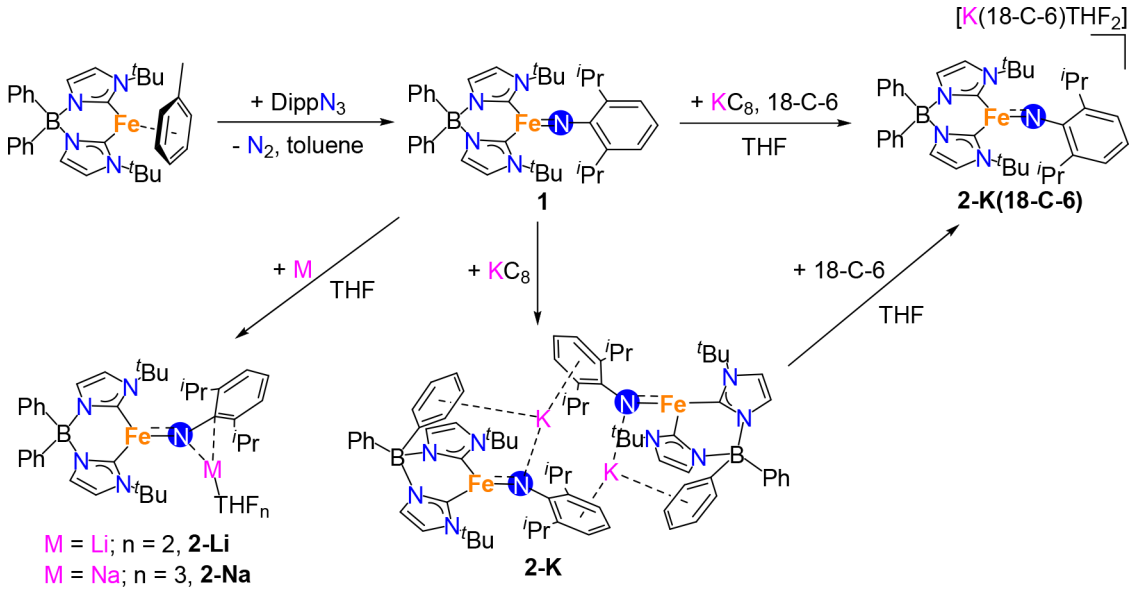

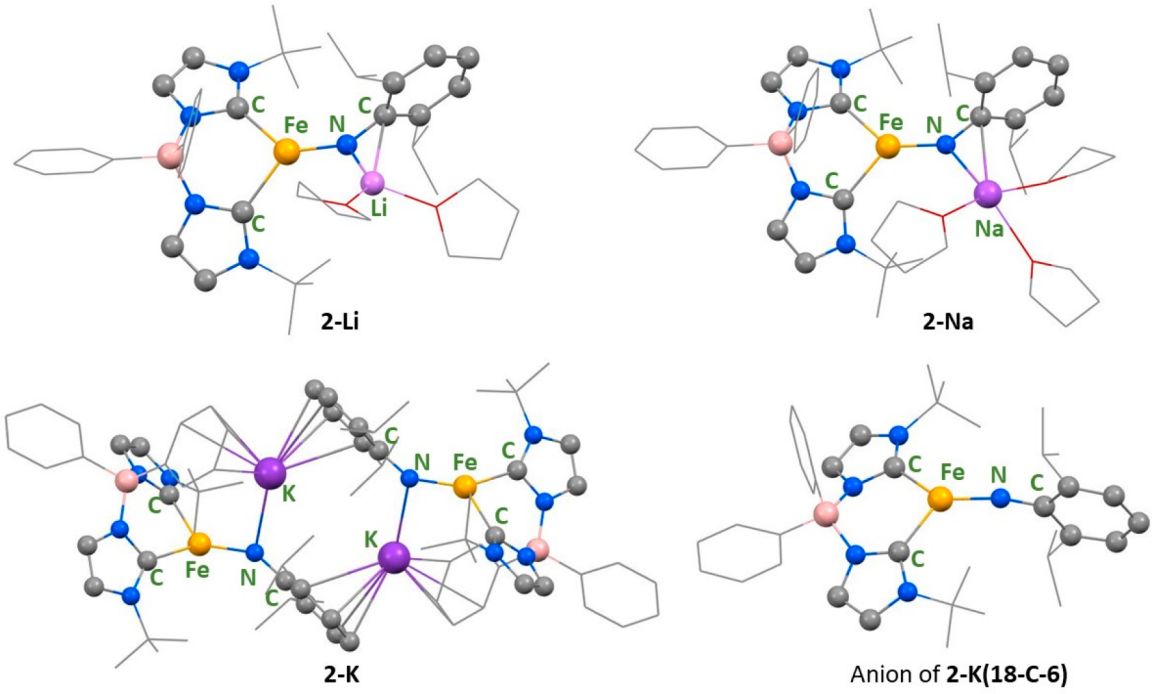

Figure 2. Molecular structures of Fe(II) imido complexes. This figure was produced on the basis of CIF files reported in refs1 and 2.

structures and unique properties in catalysis. In addition to the stoichiometric reactivity that is atypical for late transition metal complexes, the Fe═NR bond can also cooperatively facilitate unusual catalytic transformations that extend beyond nitrene transfer.

2. SYNTHESIS, CHARACTERIZATION, AND STOICHIOMETRIC REACTIVITIES OF FE(II) IMIDO COMPLEXES

2.1. Synthesis, Structural Characterization, and Electronic Structure Calculations

The entry point for this system is the Fe(III) imido complex $Ph_2B(^tBuIm)_2Fe{=}NDipp$ (**1**), which is generated by the oxidation of $Ph_2B(^tBuIm)_2Fe(I)(\eta^6\text{-toluene})$ with 1 equiv of $DippN_3$ (Scheme 1). The bulky organoazide hinders further oxidation to the Fe(V) bis(imido) complex.[45] Single crystal X-ray diffraction establishes its trigonal planar geometry with an Fe−N(imido) bond distance of 1.708(2) Å and Fe−N−C angle of 172.3(2)°, both of which are comparable to those reported in other three-coordinate Fe(III) imido complexes.[29,31] The solution magnetic moment establishes an intermediate spin (S = 3/2) Fe(III) state, which is further supported by zero field ^{57}Fe Mössbauer spectroscopy.

Reduction of **1** with alkali metals M (M = Li, Na, K) affords a series of high spin (S = 2) alkali-coordinated Fe(II) imido complexes $[Ph_2B(^tBuIm)_2Fe{=}NDippLi(THF)_2]$ (**2**-Li), $[Ph_2B(^tBuIm)_2Fe{=}NDippNa(THF)_3]$ (**2**-Na), and $[Ph_2B$-

https://doi.org/10.1021/acs.accounts.3c00511
Acc. Chem. Res. 2023, 56, 3392−3403

Table 1. Comparison of Selected Experimental and Calculated Bond Metrics in Fe(II) Imido Complexes

	2-Li		**2**-Na		**2**-K		**2**-K(18-C-6)	
	exptl.	calcd[b]	exptl.	calcd[b]	exptl.	calcd[b]	exptl.	calcd[c]
Fe−N (imido; Å)	1.8161(17)	1.829	1.812(2)	1.809	1.793(3)	1.807	1.777(2)	1.779
M···N (imido; Å)[a]	1.950(4)	1.869	2.440(3)	2.279	2.803(3)	2.644		
Fe−C (Å; average)	2.110(2)	2.085	2.097(3)	2.081	2.099(4)	2.097	2.084(2)	2.072
Fe−N−C (deg)	143.6(1)	132.7	141.5(2)	135.2	145.9(3)	131.6	172.64(19)	147.6

[a]M = Li, Na, or K. [b]Calculated for the monomeric, solvent free model complexes $[Ph_2B(^tBuIm)_2Fe{=}NDippM]$. [c]Calculated for the anion. Reprinted with permission from ref 2. Copyright 2022 American Chemical Society.

$(^tBuIm)_2Fe{=}NDippK]_2$ (**2**-K; Scheme 1). The Li^+ and Na^+ coordinated complexes have monomeric structures in which the alkali metal ion coordinates the imido nitrogen, while K^+-coordinated complex **2**-K is a dimer. The alkali metal ions in these complexes can be sequestered by crown ether; for example, the reaction of **2**-K with 1 equiv of 18-crown-6 produces the charge separated Fe(II) imido complex $[Ph_2B(^tBuIm)_2Fe{=}NDipp][K(18\text{-}C\text{-}6)THF_2]$ (**2**-K(18-C-6)), which retains the high spin configuration.

The molecular structures of these imido complexes, as determined by single crystal X-ray diffraction, reveal that the trigonal planar geometry of Fe in **1** is retained on reduction (Figure 2). The key bond metrics of these Fe(II) imido complexes are summarized in Table 1. The Fe−N(imido) bond distances in the tight ion pair complexes decrease according to **2**-Li > **2**-Na > **2**-K, in line with the relative Lewis acidities of the alkali metal ions.[46] The Fe−N(imido) distances in these complexes are all longer than those for **2**-K(18-C-6). The Fe−N(imido) bond distance in **2**-Li (1.8161(17) Å) is among the longest known and approaches that observed in the Fe(II) amido complex $Ph_2B(^tBuIm)_2FeNHDipp$ (*ca.* 1.9 Å; see below). In addition to the impact on the Fe−N(imido) bond distance, the Fe−N−C angle in **2**-Li/Na/K has a greater deviation from linearity than that in **2**-K(18-C-6), which is partly due to the interactions between the imido ligand and the alkali metal ions.

Complexes **2**-Li/Na/K and **2**-K(18-C-6) are spectroscopically distinct by ^1H NMR spectroscopy, suggesting that the solid-state structure is maintained in THF-d_8 solution. Interestingly, other spectroscopic parameters (e.g., UV−vis absorption energies and ^{57}Fe Mössbauer isomer shifts) are largely independent of the alkali metal ions, suggesting that there are only subtle effects on the electronic properties of the imido complexes. It is worth noting that cyclic voltammetry reveals the oxidation of **2**-Li (*ca.* −2.0 V vs Fc/Fc^+) is slightly more favorable than for **2**-Na/K and **2**-K(18-C-6) (*ca.* −1.9 V vs Fc/Fc^+), probably due to the more basic imido ligand of **2**-Li (see below).

Density functional theory (DFT) calculations on the THF-free model complexes $[Ph_2B(^tBuIm)_2Fe{=}NDippM]$ (M = Li, **2′**-Li; M = Na, **2′**-Na; M = K, **2′**-K) and **2** reveal that the complexes have qualitatively similar electronic structures. However, the Fe=N π-bonding orbital is polarized toward the nitrogen atom in the order **2′**-K ≈ **2′**-Na < **2′**-Li, which is further supported by NBO calculations. Consequently, the calculated imido nitrogen Mulliken charge decreases according to **2′**-Li (−0.99) > **2′**-Na ≈ **2′**-K (−0.90) > **2** (−0.71). The relative basicity of the imido ligand is expected to increase in the order **2**-K(18-C-6) < **2**-K ≈ **2**-Na < **2**-Li.

2.2. Demonstration of Imido Nucleophilicity and the Impact of the Alkali Metal Ion

The coordination of redox innocent metal ions has been proposed to modulate the properties and reactivities of metal ligand multiple bonds.[47,48] For example, the seminal work of Fukuzumi and co-workers has shown that metal ions such as Ca^{2+}, Mg^{2+}, Sc^{3+}, and Zn^{2+} can dramatically enhance the rate of electron transfer to the high-valent iron oxo complexes, as well as change the mechanism of substrate oxidation reactions.[49−51] Analogous effects might be anticipated for isoelectronic imido ligands, although there are few studies to this effect.[52] Recognizing that complexes **2**-M provide an ideal platform for these studies, we therefore became interested in delineating the impact of the alkali metal ion on the reactivity of the imido ligand.

The nucleophilic character of the imido ligand in **2**-M is readily demonstrated through protonation and alkylation reactions, where we observe that the alkali metal ion plays a vital role in directing the reactivity (Scheme 2). Specifically, the

Scheme 2. Protonation and Alkylation of the Imido Ligands in 2-M

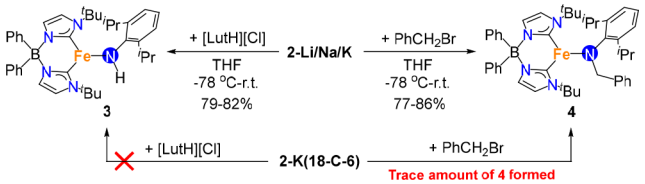

reactions of **2**-Li/Na/K with 1 equiv [LutH]Cl provides the Fe(II) amido complex $Ph_2B(^tBuIm)_2FeNHDipp$ (**3**) in high yield, whereas the same reaction with **2**-K(18-C-6) provides a complex mixture of products, with no evidence for the formation of **3**. Similarly, the reaction of **2**-Li/Na/K with 1 equiv of BnBr affords the Fe(II) amido complex $Ph_2B(^tBuIm)_2FeN(CH_2Ph)$-Dipp (**4**) in high yields. By contrast, only trace quantities of **4** are produced from **2**-K(18-C-6). These results demonstrate the effect of alkali metal ion coordination in directing these protonation and alkylation reactions, which may also be relevant to understanding the similar impact of alkali metal additives on industrial NH_3 synthesis.[53]

The nucleophilicity of **2**-M is further demonstrated through its reaction with $DippNH_2$, which establishes an equilibrium with the bis(anilido) complex $[Ph_2B(^tBuIm)_2Fe(NHDipp)_2]^-$ (**5**; Scheme 3). Importantly, ^1H NMR spectroscopy establishes that there is no interaction between the alkali metal ion and the bis(anilido) complex. The equilibrium constant for these reactions is dependent on the alkali metal ion, with K_{eq} increasing according to $Li^+ < Na^+ < K^+ < [K(18\text{-}C\text{-}6)]^+$. This suggests that the basicity for the imido ligand in the Fe(II) imido

https://doi.org/10.1021/acs.accounts.3c00511
Acc. Chem. Res. 2023, 56, 3392−3403

Scheme 3. Equilibrium Involving 5 with 2-M and DippNH$_2$ along with the Corresponding Equilibrium Constants

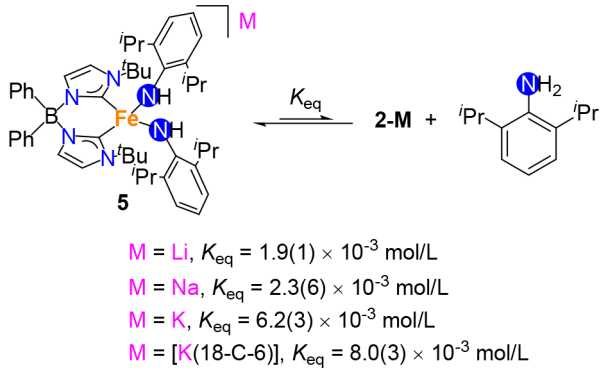

complexes decreases according to the order **2**-Li > **2**-Na > **2**-K > **2**-K(18-C-6).

The alkali metal ions significantly affect the reactivity of the imido ligand in hydrogen atom abstraction (HAA) reactions. The reaction between complex **2**-K(18-C-6) and 1,4-cyclohexadiene occurs in minutes, affording benzene along with the putative three-coordinate Fe(I) amido complex [Ph$_2$B(^{t}BuIm)$_2$FeNHDipp]$^-$ (**6**; Scheme 4). The HAA reactivity is

Scheme 4. Hydrogen Atom Abstraction Reactivity of the Imido Ligand in 2-M

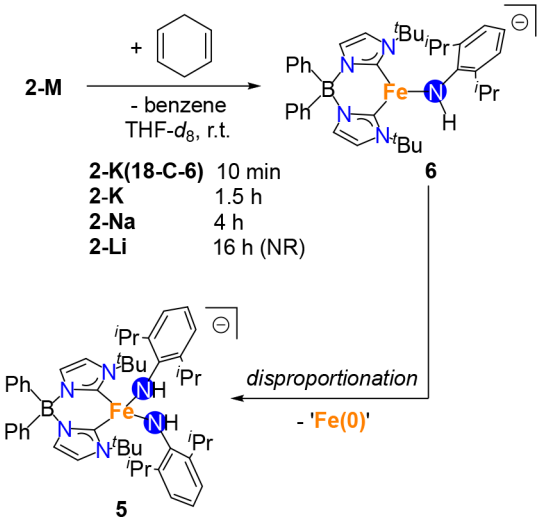

consistent with the observation of non-negligible spin density on the imido nitrogen atom (Mulliken spin density *ca.* + 0.2) in this high-spin Fe(II) imido complex. Complex **6** is unstable, ultimately producing **5**, likely via a disproportionation reaction. By contrast, **2**-Li/Na/K react considerably more slowly, with the rate decreasing in the order **2**-K > **2**-Na ≫ **2**-Li. Indeed, no reaction is observed for **2**-Li. To explain the observed different HAA reactivities, we propose that only the alkali-metal-free imido ligand can engage in the HAA reaction. The more Lewis acidic alkali metal ions bind more tightly with the imido ligand, thereby gating access to the reactive, alkali-free imido ligand and consequently decreasing the rate of HAA. This hypothesis is supported by the calculated gas phase interaction energies between alkali metal ions with the imido ligand, which follow the order $Li^+ > Na^+ > K^+$.

The alkali metal ions also influence the reaction with unsaturated electrophiles. For example, the reaction of **2**-K(18-C-6) with 1 equiv of Ph$_2$CO affords a spectroscopically characterized product that we propose to be the [2 + 2] cycloaddition product [Ph$_2$B(^{t}BuIm)$_2$Fe(N(Dipp)C(Ph)$_2$O)]-[K(18-C-6)] (**7**; Scheme 5). This complex is not stable and

Scheme 5. Reactions of 2-M with Ph$_2$CO

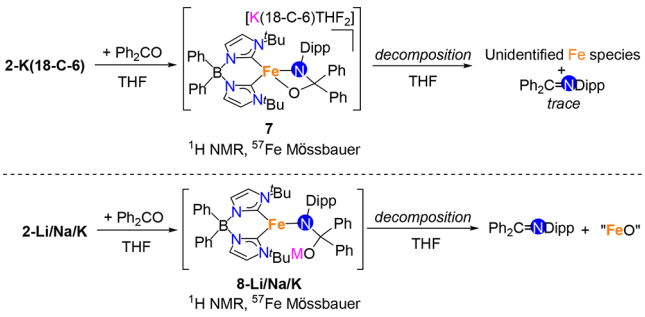

decomposes to multiple unknown iron species, along with trace amounts of the imine Ph$_2$C=NDipp. By contrast, the reactions of **2**-Li/Na/K with Ph$_2$CO form the spectroscopically characterized three-coordinate iron amido species [Ph$_2$B(^{t}BuIm)$_2$FeN(Dipp)C(Ph)$_2$OM(THF)$_x$] (**8**, M = Li, Na, K), in which the alkali metal ion coordinates to the oxygen atom. As with **7**, complexes **8** are also unstable, but now decomposition cleanly yields the imine Ph$_2$C=NDipp along with a putative iron(II) oxo. We suggest that imine formation is likely driven by the electrostatic stabilization of the iron oxo product by the alkali metal ion. Sequestration of K^+ by 18-C-6 in **7** removes this driving force, leading to a low yield of imine. Notably, we did not observe the putative iron(II) oxo product in this reaction. Interestingly, the rates of decomposition of **8** are dependent on the alkali metal ions with k_{obs} (**8**-K) ≈ k_{obs} (**8**-Na) > k_{obs} (**8**-Li). In this case, we propose that the more Lewis acidic Li^+ stabilizes **8** through stronger coordination to the oxygen atom of this intermediate.

Together, these stoichiometric reactions reveal that the imido ligand in complexes **2**-M has a nucleophilic character. We recognized that the unusual combination of a nucleophilic imido ligand and late metal center may allow these complexes to facilitate new metal imido catalysis.

3. CATALYTIC TRANSFORMATIONS MEDIATED BY FE(II) IMIDO COMPLEXES

Our initial investigations were based on our expectation that **2**-M may show catalytic reactivity similar to that of early metal complexes. Indeed, as described in more detail below, this is true in at least one instance, although the activity occurs under milder conditions and with greater substrate scope. More interestingly, subsequent investigations uncovered an unusual mode of activity for an imido complex, where the iron center and imido ligand cooperatively catalyze reactions that involve the redistribution of protons.

3.1. Catalytic Carbodiimide Guanylation

Taking a page from early transition metal imido catalysis, we initially investigated [2 + 2] cycloaddition catalysis, specifically the catalytic guanylation of carbodiimides. Complex **2**-K(18-C-6) reacts with 1 equiv of ^{i}PrN=C=N^{i}Pr to provide the crystallographically characterized high-spin complex [Ph$_2$B(^{t}BuIm)$_2$Fe(^{i}PrN)$_2$CNDipp][K(18-C-6)THF$_2$] (**9**; Scheme

https://doi.org/10.1021/acs.accounts.3c00511
Acc. Chem. Res. 2023, 56, 3392−3403

6), which results from the formal insertion of ^{i}PrN=C=N^{i}Pr into the Fe=NR bond. The outcome of this reaction differs

Scheme 6. Establishing a Catalytic Cycle for Fe(II) Imido Catalyzed Carbodiimide Guanylation

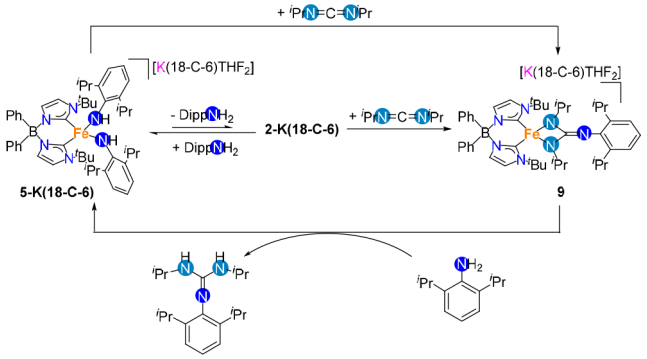

from that typically observed, which involves the [2 + 2] cycloaddition of the metal imido with carbodiimide.[21] The formation of **9** can be rationalized according to [2 + 2] cycloaddition between ^{i}PrN=C=N^{i}Pr and Fe=NR, which is followed by 1,3-Fe migration. It is worth noting here that carbodiimides are more typically the *products* of catalysis for late metal imido complexes and are usually formed by nitrene transfer chemistry to isonitriles.[22]

We found that complex **9** reacts with excess $DippNH_2$ to generate the bis(anilido) complex **5**-K(18-C-6) concomitant with guanidine (^{i}PrNH)$_2$C=NDipp (Scheme 6). Since we had established that **5**-K(18-C-6) is in equilibrium with the imido **2**-K(18-C-6) in solution (see above), it was not surprising (although still gratifying) to observe that **5**-K(18-C-6) readily reacts with excess ^{i}PrN=C=N^{i}Pr to regenerate **9**. Together, these stoichiometric transformations suggested that **2**-K(18-C-6) would be a catalyst for the guanylation of carbodiimides.

At 5 mol % loading, **2**-K(18-C-6) is an effective catalyst for converting a range of anilines and carbodiimides to guanidines (Table 2). Compared to early transition metal imido complexes,[54] in which heating is usually required, the mild conditions for catalysis by **2**-K(18-C-6) are notable. We also observed the catalyst to have good functional group tolerance; e.g., anilines containing reactive trifluoromethyl, cyanide, ester, and sulfonyl groups are suitable substrates. We suggest both of these properties can be attributed at least in part to the high spin state of the Fe center in **2**-K(18-C-6). Specifically, all 3d orbitals are at least singly occupied, which imparts greater substrate and product lability as well as leads to weaker interactions with Lewis basic poisons.[55]

A number of observations suggest that the imido ligand plays a key role in the catalytic mechanism. We note that the rate of the reaction is considerably slower when **5**-K(18-C-6) is used as the catalyst. In addition, catalysis is shut down by excess $DippNH_2$. We therefore suggest that catalysis occurs by the mechanism shown in Scheme 7. The Fe(II) imido complex A reacts with the carbodiimide substrate to provide guanidinate complex B (structurally characterized as **9**) followed by reaction with 1 equiv of aniline to yield intermediate C. The mechanism bifurcates at this point with intramolecular proton transfer releasing the guanidine product (path a), which regenerates A and completes the catalytic cycle. Alternatively, another equivalent of aniline reacts with C to generate a guanidine product with concomitant formation of bis(anilido) complex D

Table 2. Substrate Scope of Catalytic Carbodiimide Guanylation

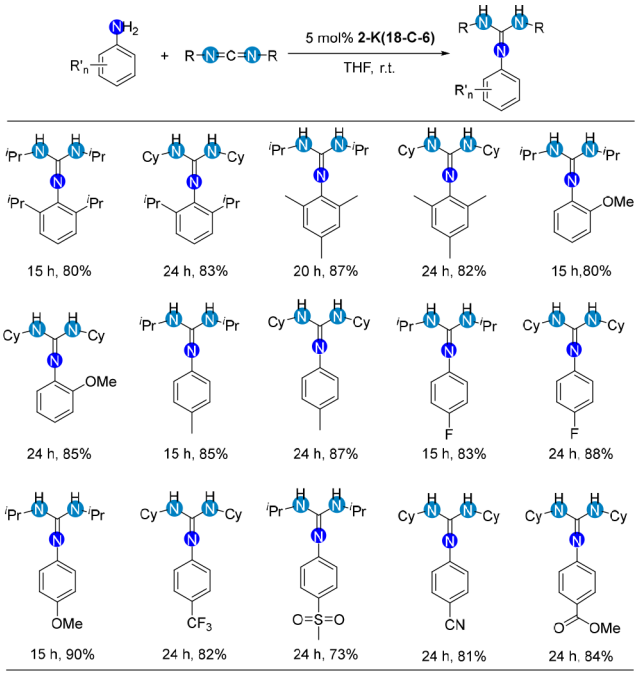

Scheme 7. Proposed Mechanism for Fe(II) Imido Catalyzed Carbodiimide Guanylation

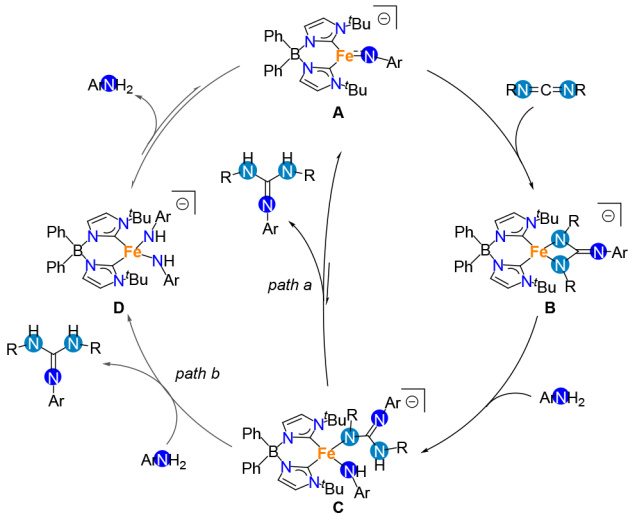

(path b), which we know to be in equilibrium with A. We suggest that path a is more likely because the rate of reaction is slower when **5**-K(18-C-6) is used as the catalyst instead of **2**-K(18-C-6) or **9**.

3.2. Catalytic α-Deuteration of Nitriles and Alkynes

Since complexes **2**-M provide a coordinatively unsaturated metal center with a strong donor supporting ligand, we hypothesized that they may react with π-acidic substrates such as alkynes. Metal imido complexes have been shown to react with internal alkynes, typically via a [2 + 2] cycloaddition reaction to afford four-membered metallacycle complexes.[21] Unexpectedly, we observe that **2**-K(18-C-6) reacts with 1 equiv of EtC≡CEt to provide Fe(II) amido allenyl complex **10** (Scheme 8). Other internal alkynes react similarly, including

https://doi.org/10.1021/acs.accounts.3c00511
Acc. Chem. Res. 2023, 56, 3392−3403

Scheme 8. Reaction of Fe(II) Imido Complexes with Alkynes and Nitriles

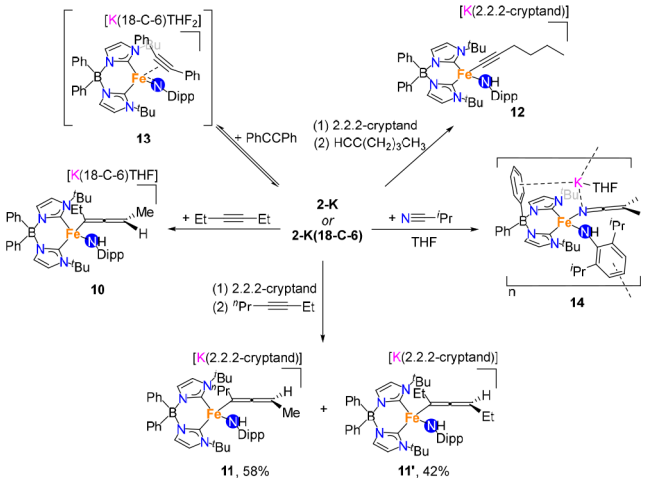

unsymmetric substrate ^{n}PrC≡CEt, which affords two isomers (**11** and **11′**). These reactions are analogous to those of strong bases such as ^{n}BuLi, which facilitates isomerization to allenes through the α-deprotonation of alkynes.[56] Similar reactivity of **2**-M with terminal alkynes is not observed; e.g., 1-hexyne yields the Fe(II) amido alkynyl complex **12**, which is likely due to the greater acidity of the C(sp)−H bond in 1-hexyne. In the case of 1 equiv of diphenylacetylene, which lacks an α-C−H bond, ^{1}H NMR spectroscopy suggests that an equilibrium between **2**-K(18-C-6), PhC≡CPh, and the η^2-alkyne coordinated complex **13** is established ($K_{eq} \approx 0.2$ mol/L).

Formally, the formation of **10**, **11**, and **11′** occur *via* ene reactions of the Fe═NR bond, a previously unobserved transformation for transition metal−ligand multiple bonds, including imidos. While ene reactions of organic substrates generally follow a concerted mechanism,[57] we propose a stepwise pathway in which η^2-coordination to the imido enables subsequent α-proton transfer to the basic imido ligand and isomerization to yield the allenyl products. This ene-like reactivity can be extended to nitriles; e.g., isobutyronitrile reacts to provide the Fe(II) amido keteniminate complex **14**.

DFT calculations suggest that the γ-carbon of the allenyl ligand and β-carbon of the keteniminate ligand have nucleophilic character.[58,59] Consistent with this, we observe that amines protonate these carbon atoms to generate 3-hexyne and isobutyronitrile with concomitant formation of the respective bis(amido) complexes (Scheme 9). Since these are in equilibrium with the Fe(II) imido complex, we recognized that we could develop a catalytic cycle for the selective α-deuteration of internal alkynes and nitriles by Fe(II) imido complex **2**-K(18-C-6) (Scheme 10).

Scheme 9. Elementary Steps Towards Catalytic α-Deuteration of Internal Alkynes and Nitriles

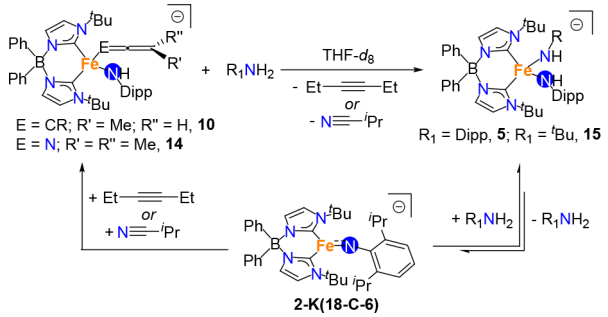

Scheme 10. Catalytic Cycle for Selective α-Deuteration by an Fe(II) Imido Complex with ^{t}BuND$_2$ as the Deuterium Source

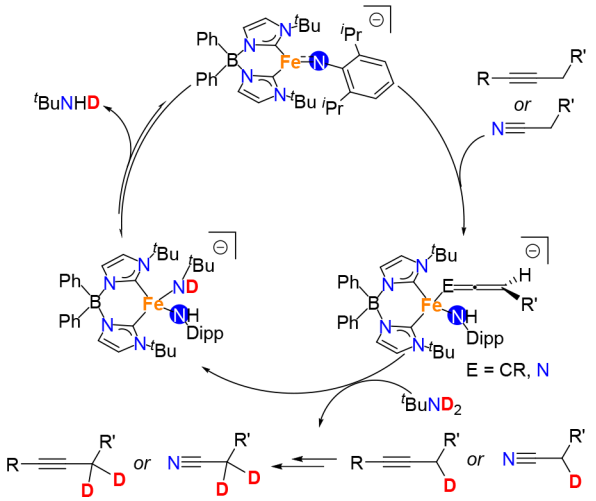

Gratifyingly, we found that a series of aliphatic nitriles are successfully α-deuterated with 2 mol % **2**-K(18-C-6) in the presence of 20 equiv of ^{t}BuND$_2$ at room temperature (Table 3). More interestingly, **2**-K(18-C-6) catalytically α-deuterates internal alkynes, although higher catalyst loadings (5 mol %) and gentle heating is required. For unsymmetric alkynes, we observe exclusive deuteration of the methyl group while the more sterically inaccessible α-methylene remains untouched. Interestingly, the catalytic α-deuteration of alkyl-substituted alkynes requires the use of ^{n}PrND$_2$ as the deuterium source, likely due to the greater steric constraints of the alkyl chain.

Table 3. Substrate Scope of Catalytic α-Deuteration of Internal Alkynes and Nitriles

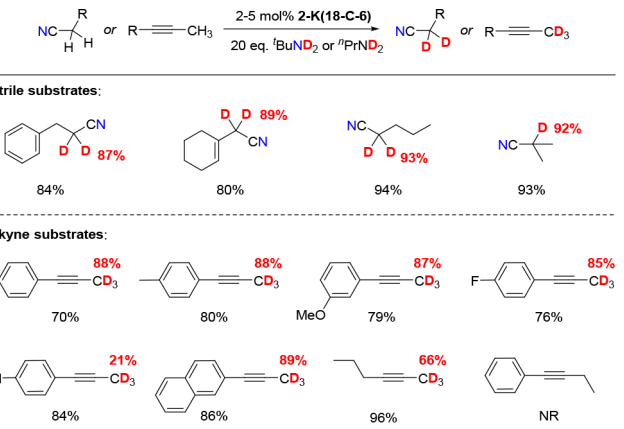

3.3. pK_a-Dictated Alkene Transposition

The reactivity of the Fe(II) imido complex with alkynes and nitriles involves proton transfer to the imido ligand, suggesting to us that other compounds with weakly acidic protons may also be suitable substrates for catalytic transformations, including alkenes with sufficiently acidic allyl protons. Indeed, it has been known for over 50 years that strong bases can effect double bond

https://doi.org/10.1021/acs.accounts.3c00511
Acc. Chem. Res. 2023, 56, 3392−3403

transposition in substrates such as allylbenzenes.[60,61] Translating this reactivity to the Fe(II) imido complex would likely entail a novel, nonhydridic mechanism for transition metal-catalyzed double bond transposition. Moreover, it might be expected that such a mechanism would provide a means for controlling substrate regioselectivity through pK_a of the allylic proton.

Table 4. Catalytic Transposition of Allylbenzenes by 2-K(18-C-6)

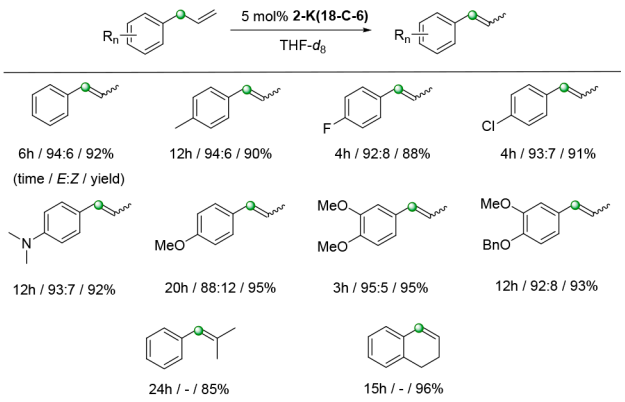

We first tested for double bond transposition in allylbenzenes, which have relatively acidic allylic protons (pK_a ≈ 33 for allylbenzene in DMSO).[62] Gratifyingly, we observe that a range of allylbenzenes are successfully transposed to the corresponding prop-1-en-1-ylbenzene products using 5 mol % **2**-K(18-C-6) as a catalyst (Table 4). The transposed products are obtained in high yields under mild conditions. As with many other transition metal catalysts,[63] transposition occurs with selectivity for the *E* isomer. Encouragingly, transposition is successful for more sterically hindered 1,1-disubstituted and internal allylbenzenes. It is worth noting that there is no evidence for the formation of naphthalene from 1,4-dihydronaphthalene, indicating that catalysis does not involve hydrogen atom abstraction.

Mechanistic investigations used allylbenzene as a model substrate. Here, we observed that transposition is inhibited by equimolar 1-octene or *cis*-stilbene (Figure 3a), neither of which is a substrate for transposition catalysis, implicating alkene coordination to Fe. Furthermore, the rate of transposition is strongly dependent on the identity of the alkali counterion, with the rate decreasing according to **2**-K(18-C-6) > **2**-K > **2**-Na ≫ **2**-Li (Figure 3b). Since the imido ligand is sequestered by more Lewis acidic alkali ions (see above), this suggests that the imido ligand is critical to catalysis. These results also indicate that the interaction between the imido nitrogen and alkali metal in **2**-Li/Na/K needs to be broken before the imido ligand can interact with the alkene substrates.

The rate of double bond transposition is notably slower when allylbenzene is selectively deuterated at the benzylic positions (k_H/k_D = 34 at 40 °C; Scheme 11a). Combined with the results of a crossover experiment (Scheme 11b), these results are consistent with a mechanism involving an intramolecular 1,3-proton transfer step. This is further supported by the Hammett plot for the transposition of a series of *para*-substituted allylbenzenes, where the positive slope (ρ = 1.54) implicates proton transfer (Figure 4).

Stoichiometric experiments also provide insight into the catalytic mechanism. Here, we observe that **2**-K(18-C-6) reacts

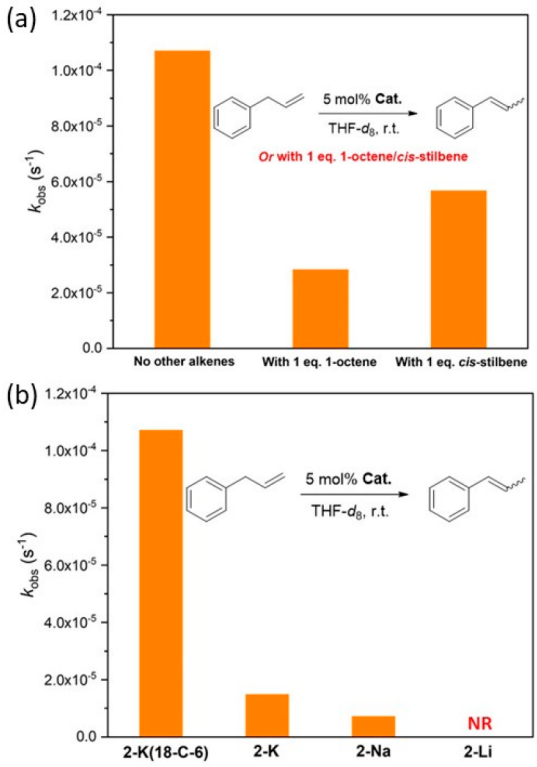

Figure 3. (a) Comparison of rate constants for catalytic transposition of allylbenzene in the presence of 1-octene or *cis*-stilbene using **2**-K(18-C-6) as the catalyst. (b) Comparison of rate constants for catalytic transposition of allylbenzene using **2**-K(18-C-6) and **2**-Li/Na/K as the catalysts. Reprinted with permission from ref 4. Copyright 2023 American Chemical Society.

Scheme 11. Deuterium Labeling Studies

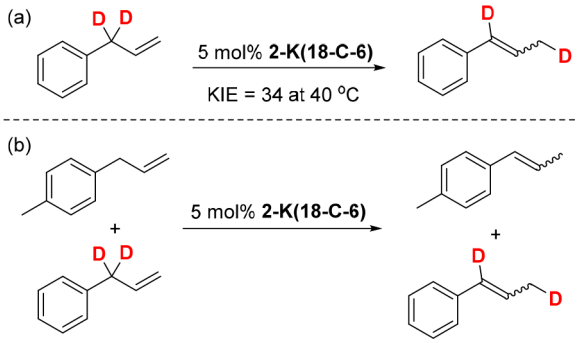

with 1 equiv of allylbenzene to form a metastable complex tentatively assigned as the Fe(II) η^1-allyl amido complex $[Ph_2B(^tBuIm)_2Fe(NHDipp)(\eta^1\text{-}H_2CC(H)=C(H)Ph)]^-$ (**16**) on the basis of its spectroscopic properties and chemical reactivity (Scheme 12). Importantly, Fe(I) amido species **6** is not observed, suggesting the reaction involves proton and not hydrogen atom abstraction. In addition, complex **16** also serves as a catalyst for transposition of allylbenzene with the rate and *E* to *Z* selectivity being the same as for **2**-K(18-C-6).

Based on these observations, we propose the alkene transposition shown in Scheme 13. First, the alkene binds to the Fe center of the imido complex, yielding intermediate A′. Subsequent transfer of the allylic proton to the imido ligand is accompanied by double bond transposition to afford intermediate B′. Finally, intramolecular α-elimination from B′

https://doi.org/10.1021/acs.accounts.3c00511
Acc. Chem. Res. 2023, 56, 3392−3403

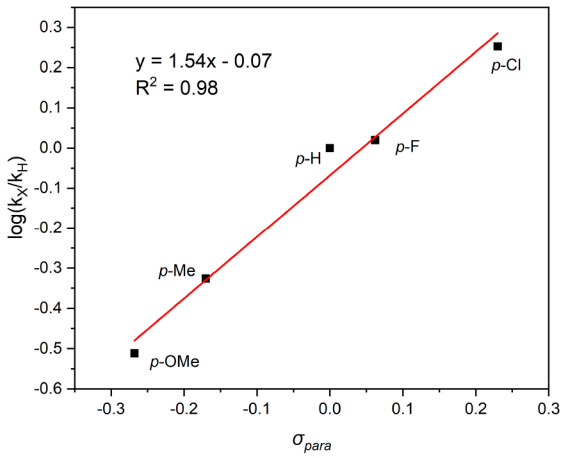

Figure 4. Hammett plot for the transposition of a series of *para*-substituted allylbenzenes using 5 mol % **2**-K(18-C-6) as the catalyst. Reprinted with permission from ref 4. Copyright 2023 American Chemical Society.

Scheme 12. Stoichiometric Reaction of 2-K(18-C-6) with Allylbenzene and the Subsequent Reaction with Amines

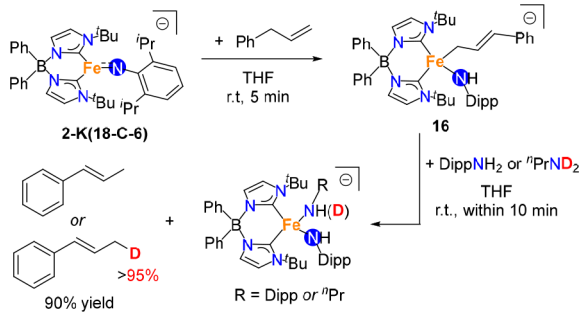

Scheme 13. Catalytic Cycle for Alkene Transposition by 2-K(18-C-6)

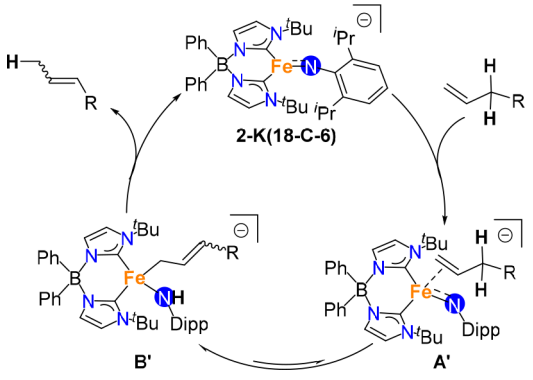

produces the transposed alkene, regenerating the Fe(II) imido complex and closing the catalytic cycle. It is notable that this mechanism does not require iron hydride intermediates. DFT calculations support the proposed mechanism and suggest that the second intramolecular proton transfer is the rate-determining step. These calculations also suggest that catalysis occurs only on the quintet spin surface.

Complex **2**-K(18-C-6) also catalyzes the transposition of a series of nonbenzylic alkenes as listed in Table 5. However, less acidic alkenes are inactive as substrates. Based on the theoretically predicted pK_a values for these compounds,

Table 5. pK_a Dictated Alkene Transposition by 2-K(18-C-6)

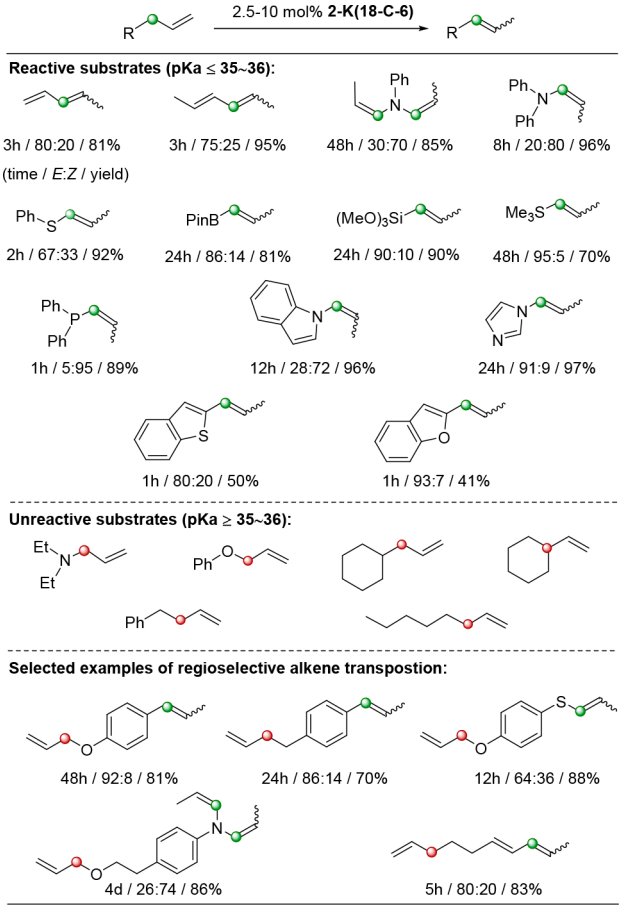

transposition occurs when the pK_a of the allylic protons is less than 35−36. This pK_a-dictated reactivity enables the predicable regioselective transposition of a series of substrates containing multiple 1-alkene functionalities. Similar regioselectivity is not observed for transition metal catalysts that involve hydride intermediates.

4. CONCLUSION AND OUTLOOK

The aforementioned investigations demonstrate the critical role that supporting ligands play in dictating the reactivity of the imido ligand in an iron complex. Here, the strongly electron donating bis(carbene)borate ligand stabilizes a nucleophilic three-coordinate high-spin Fe(II) imido complex whose reactivity differs significantly from that of classical nitrene transfer chemistry.

The high negative charge density on the imido ligand in the Fe(II) complex is structurally demonstrated through its interactions with alkali metal ions with more Lewis acidic ions binding more tightly to the imido ligand. The properties of the imido ligand (e.g., basicity) are greatly affected by the presence of alkali metal ions. The alkali metal ions also play a critical role in determining the outcome of protonation and alkylation reactions as well as the rate of hydrogen atom abstraction. Moreover, the alkali metal ions dictate the outcome of double bond metathesis with Ph_2CO, likely by stabilizing reaction intermediates.

The nucleophilic nature of the imido ligand allows for a proton transfer equilibrium involving the Fe(II) imido complex, a bulky aniline, and a bis(anilido) complex. This equilibrium

https://doi.org/10.1021/acs.accounts.3c00511
Acc. Chem. Res. 2023, 56, 3392−3403

enables the development of catalytic transformations that stem from the stoichiometric reactivity of the imido ligand. For example, a stoichiometric [2 + 2] cycloaddition reaction between the Fe═NR bond and a carbodiimide provides the basis for catalytic carbodiimide guanylation. More interestingly, the nucleophilic character of the imido ligand enables unprecedented ene-like reactivity with internal alkynes, nitriles, and alkenes. These transformations form the basis of catalytic α-deuteration of internal alkynes and nitriles and pK_a-dictated alkene transposition, respectively. Our mechanistic studies reveal the critical role of metal−ligand cooperativity in facilitating these unusual transformations. Interestingly, despite the greater basicity of the imido ligand in **2**-Li/Na/K, the electrostatic interaction with alkali metal ions hinders substrate access and decreases their activity in catalysis reactivity, in comparison with **2**-K(18-C-6).

We envision that the unusual nucleophilicity of the imido ligand can be extended to other transformations that go beyond classical nitrene transfer chemistry. For example, it is likely that Fe═NR bond cooperativity can be applied to other chemical bonds such as H−H, H-SiR_3, and H-BR_2, which would provide the basis for catalytic hydrogenation, hydrosilylation, or hydroboration. More ambitiously, with appropriate ligand tailoring, we envision that the pK_a-dictated substrate activity can be applied to site selective C−H bond activation and functionalization. Finally, we anticipate that our strategy for creating a highly nucleophilic imido ligand can be extended to other late transition metals, which may lead to a greater diversity of imido reactivity

AUTHOR INFORMATION

Corresponding Authors

Yafei Gao − *Department of Chemistry, Indiana University, Bloomington, Indiana 47405, United States;* orcid.org/0000-0001-7970-8535; Email: gaoyafe@iu.edu

Jeremy M. Smith − *Department of Chemistry, Indiana University, Bloomington, Indiana 47405, United States;* orcid.org/0000-0002-3206-4725; Email: smith962@indiana.edu

Complete contact information is available at: https://pubs.acs.org/10.1021/acs.accounts.3c00511

Author Contributions

The authors declare no competing financial interest. CRediT: **Yafei Gao** conceptualization, data curation, formal analysis, investigation, validation, visualization, writing-original draft, writing-review & editing; **Jeremy M. Smith** conceptualization, data curation, formal analysis, funding acquisition, methodology, project administration, supervision, validation, visualization, writing-original draft, writing-review & editing.

Notes

The authors declare no competing financial interest.

Biographies

Yafei Gao grew up in Henan, China. He received his B.S. degree from Central South University in 2013. He then joined Shanghai Institute of Organic Chemistry, Chinese Academy Sciences, and received his Ph.D. degree in 2018 under the supervision of Prof. Liang Deng. In 2019, he moved to Indiana University Bloomington and worked as a postdoctoral fellow with Prof. Jeremy M. Smith. From August 2023, he has continued as a postdoctoral fellow with Prof. Jose M. Goicoechea at the same university.

Jeremy M. Smith was raised in Benoni, South Africa. He completed both undergraduate and graduate studies at the University of the Witwatersrand, where he obtained his Ph.D. under the supervision of Neil J. Coville. Following postdoctoral stints with Russell P. Hughes (Dartmouth College) and Patrick L. Holland (University of Rochester), he started his independent career at New Mexico State University in 2003. He moved to Indiana University in 2013, where he is currently Professor of Chemistry.

ACKNOWLEDGMENTS

This material is based upon work supported by the U.S. Department of Energy, Office of Science, Office of Basic Energy Sciences under Award Number DE-SC0019466. We also thank the NSF for financial support (OMA-1936353).

REFERENCES

(1) Gao, Y.; Carta, V.; Pink, M.; Smith, J. M. Catalytic Carbodiimide Guanylation by a Nucleophilic, High Spin Iron(II) Imido Complex. *J. Am. Chem. Soc.* **2021**, *143*, 5324−5329.

(2) Gao, Y.; Pink, M.; Smith, J. M. Alkali Metal Ions Dictate the Structure and Reactivity of an Iron(II) Imido Complex. *J. Am. Chem. Soc.* **2022**, *144*, 1786−1794.

(3) Gao, Y.; Pink, M.; Carta, V.; Smith, J. M. Ene Reactivity of an Fe═NR Bond Enables the Catalytic α-Deuteration of Nitriles and Alkynes. *J. Am. Chem. Soc.* **2022**, *144*, 17165−17172.

(4) Gao, Y.; Li, X.; Stevens, J. E.; Tang, H.; Smith, J. M. Catalytic 1,3-Proton Transfer in Alkenes Enabled by Fe═NR Bond Cooperativity: A Strategy for pKa-Dictated Regioselective Transposition of C═C Double Bonds. *J. Am. Chem. Soc.* **2023**, *145*, 11978−11987.

(5) Crawley, M. L.; Trost, B. M. *Applications of Transition Metal Catalysis in Drug Discovery and Development*; John Wiley & Sons: Hoboken, 2012.

(6) Xia, Y.; Qiu, D.; Wang, J. Transition-Metal-Catalyzed Cross-Couplings through Carbene Migratory Insertion. *Chem. Rev.* **2017**, *117*, 13810−13889.

(7) Zweig, J. E.; Kim, D. E.; Newhouse, T. R. Methods Utilizing First-Row Transition Metals in Natural Product Total Synthesis. *Chem. Rev.* **2017**, *117*, 11680−11752.

(8) Roh, S. W.; Choi, K.; Lee, C. Transition Metal Vinylidene- and Allenylidene-Mediated Catalysis in Organic Synthesis. *Chem. Rev.* **2019**, *119*, 4293−4356.

(9) Yang, H.; Yu, H.; Stolarzewicz, I. A.; Tang, W. Enantioselective Transformations in the Synthesis of Therapeutic Agents. *Chem. Rev.* **2023**, *123*, 9397−9446.

(10) Mo, Z.; Deng, L. Open-Shell Iron Hydrocarbyls. *Coord. Chem. Rev.* **2017**, *350*, 285−299.

(11) Neidig, M. L.; Carpenter, S. H.; Curran, D. J.; DeMuth, J. C.; Fleischauer, V. E.; Iannuzzi, T. E.; Neate, P. G. N.; Sears, J. D.; Wolford, N. J. Development and Evolution of Mechanistic Understanding in Iron-Catalyzed Cross-Coupling. *Acc. Chem. Res.* **2019**, *52*, 140−150.

(12) Jung, H.; Kweon, J.; Suh, J. M.; Lim, M. H.; Kim, D.; Chang, S. Mechanistic Snapshots of Rhodium-catalyzed Acylnitrene Transfer Reactions. *Science* **2023**, *381*, 525−532.

(13) Sun, J.; Deng, L. Cobalt Complex-Catalyzed Hydrosilylation of Alkenes and Alkynes. *ACS Catal.* **2016**, *6*, 290−300.

(14) Alig, L.; Fritz, M.; Schneider, S. First-Row Transition Metal (De)Hydrogenation Catalysis Based On Functional Pincer Ligands. *Chem. Rev.* **2019**, *119*, 2681−2751.

(15) Elsby, M. R.; Baker, R. T. Strategies and Mechanisms of Metal-ligand Cooperativity in First-row Transition Metal Complex Catalysts. *Chem. Soc. Rev.* **2020**, *49*, 8933−8987.

(16) Wigley, D. E. Organoimido Complexes of the Transition Metals. *Prog. Inorg. Chem.* **1994**, *42*, 239−482.

(17) Zhang, L.; Deng, L. C-H Bond Amination by Iron-Imido/Nitrene Species. *Chin. Sci. Bull.* **2012**, *57*, 2352−2360.
(18) Wang, P.; Deng, L. Recent Advances in Iron-Catalyzed C-H Bond Amination via Iron Imido Intermediate. *Chin. J. Chem.* **2018**, *36*, 1222−1240.
(19) Grünwald, A.; Anjana, S. S.; Munz, D. Terminal Imido Complexes of the Groups 9−11: Electronic Structure and Developments in the Last Decade. *Eur. J. Inorg. Chem.* **2021**, *2021*, 4147−4166.
(20) Anderson, J. S.; Rittle, J.; Peters, J. C. Catalytic Conversion of Nitrogen to Ammonia by an Iron Model Complex. *Nature* **2013**, *501*, 84−87.
(21) Kawakita, K.; Kakiuchi, Y.; Tsurugi, H.; Mashima, K.; Parker, B. F.; Arnold, J.; Tonks, I. A. Reactivity of Terminal Imido Complexes of Group 4−6 Metals: Stoichiometric and Catalytic Reactions Involving Cycloaddition with Unsaturated Organic Molecules. *Coord. Chem. Rev.* **2020**, *407*, No. 213118.
(22) Cowley, R. E.; Eckert, N. A.; Elhaik, J.; Holland, P. L. Catalytic Nitrene Transfer from an Imidoiron(III) Complex to form Carbodiimides and Isocyanates. *Chem. Commun.* **2009**, 1760−1762.
(23) Hennessy, E. T.; Liu, R. Y.; Iovan, D. A.; Duncan, R. A.; Betley, T. A. Iron-Mediated Intermolecular N-Group Transfer Chemistry with Olefinic Substrates. *Chem. Sci.* **2014**, *5*, 1526−1532.
(24) Wang, B.; Seo, C. S. G.; Zhang, C.; Chu, J.; Szymczak, N. K. A Borane Lewis Acid in the Secondary Coordination Sphere of a Ni(II) Imido Imparts Distinct C-H Activation Selectivity. *J. Am. Chem. Soc.* **2022**, *144*, 15793−15802.
(25) Eckert, N. A.; Vaddadi, S.; Stoian, S.; Lachicotte, R. J.; Cundari, T. R.; Holland, P. L. Coordination-Number Dependence of Reactivityin an Imidoiron(III) Complex. *Angew. Chem., Int. Ed.* **2006**, *45*, 6868−6871.
(26) Cowley, R. E.; DeYonker, N. J.; Eckert, N. A.; Cundari, T. R.; DeBeer, S.; Bill, E.; Ottenwaelder, X.; Flaschenriem, C.; Holland, P. L. Three-Coordinate Terminal Imidoiron(III) Complexes: Structure, Spectroscopy, and Mechanism of Formation. *Inorg. Chem.* **2010**, *49*, 6172−6187.
(27) Cowley, R. E.; Eckert, N. A.; Vaddadi, S.; Figg, T. M.; Cundari, T. R.; Holland, P. L. Selectivity and Mechanism of Hydrogen Atom Transfer by an Isolable Imidoiron(III) Complex. *J. Am. Chem. Soc.* **2011**, *133*, 9796−9811.
(28) Cowley, R. E.; Holland, P. L. C−H Activation by a Terminal Imidoiron(III) Complex to Form a Cyclopentadienyliron(II) Product. *Inorg. Chim. Acta* **2011**, *369*, 40−44.
(29) Cowley, R. E.; Holland, P. L. Ligand Effects on Hydrogen Atom Transfer from Hydrocarbons to Three-Coordinate Iron Imides. *Inorg. Chem.* **2012**, *51*, 8352−8361.
(30) Hennessy, E. T.; Betley, T. A. Complex N-Heterocycle Synthesis via Iron-Catalyzed, Direct C−H Bond Amination. *Science* **2013**, *340*, 591−595.
(31) Wilding, M. J. T.; Iovan, D. A.; Betley, T. A. High-Spin Iron Imido Complexes Competent for C-H Bond Amination. *J. Am. Chem. Soc.* **2017**, *139*, 12043−12049.
(32) Wilding, M. J. T.; Iovan, D. A.; Wrobel, A. T.; Lukens, J. T.; MacMillan, S. N.; Lancaster, K. M.; Betley, T. A. Direct Comparison of C-H Bond Amination Efficacy through Manipulation of Nitrogen-Valence Centered Redox: Imido versus Iminyl. *J. Am. Chem. Soc.* **2017**, *139*, 14757−14766.
(33) Cowley, R. E.; Bontchev, R. P.; Sorrell, J.; Sarracino, O.; Feng, Y.; Wang, H.; Smith, J. M. Formation of a Cobalt(III) Imido from a Cobalt(II) Amido Complex. Evidence for Proton-Coupled Electron Transfer. *J. Am. Chem. Soc.* **2007**, *129*, 2424−2425.
(34) Nieto, I.; Ding, F.; Bontchev, R. P.; Wang, H.; Smith, J. M. Thermodynamics of Hydrogen Atom Transfer to a High-Valent Iron Imido Complex. *J. Am. Chem. Soc.* **2008**, *130*, 2716−2717.
(35) Scepaniak, J. J.; Fulton, M. D.; Bontchev, R. P.; Duesler, E. N.; Kirk, M. L.; Smith, J. M. Structural and Spectroscopic Characterization of an Electrophilic Iron Nitrido Complex. *J. Am. Chem. Soc.* **2008**, *130*, 10515−10517.
(36) Scepaniak, J. J.; Vogel, C. S.; Khusniyarov, M. M.; Heinemann, F. W.; Meyer, F.; Smith, J. M. Synthesis, Structure, and Reactivity of an Iron(V) Nitride. *Science* **2011**, *331*, 1049−1052.
(37) Smith, J. M.; Mayberry, D. E.; Margarit, C. G.; Sutter, J.; Wang, H.; Meyer, K.; Bontchev, R. P. N-O bond Homolysis of an Iron(II) TEMPO Complex Yields an Iron(III) Oxo Intermediate. *J. Am. Chem. Soc.* **2012**, *134*, 6516−6519.
(38) Lin, H. J.; Siretanu, D.; Dickie, D. A.; Subedi, D.; Scepaniak, J. J.; Mitcov, D.; Clerac, R.; Smith, J. M. Steric and Electronic Control of the Spin State in Three-fold Symmetric, Four-coordinate Iron(II) Complexes. *J. Am. Chem. Soc.* **2014**, *136*, 13326−13332.
(39) Munoz, S. B.; Lee, W. T.; Dickie, D. A.; Scepaniak, J. J.; Subedi, D.; Pink, M.; Johnson, M. D.; Smith, J. M. Styrene Aziridination by Iron(IV) Nitrides. *Angew. Chem., Int. Ed.* **2015**, *54*, 10600−10603.
(40) Martinez, J. L.; Lin, H. J.; Lee, W. T.; Pink, M.; Chen, C. H.; Gao, X.; Dickie, D. A.; Smith, J. M. Cyanide Ligand Assembly by Carbon Atom Transfer to an Iron Nitride. *J. Am. Chem. Soc.* **2017**, *139*, 14037−14040.
(41) Valdez-Moreira, J. A.; Beagan, D. M.; Yang, H.; Telser, J.; Hoffman, B. M.; Pink, M.; Carta, V.; Smith, J. M. Hydrocarbon Oxidation by an Exposed, Multiply Bonded Iron(III) Oxo Complex. *ACS Cent. Sci.* **2021**, *7*, 1751−1755.
(42) Du, J.; Wang, L.; Xie, M.; Deng, L. A Two-Coordinate Cobalt(II) Imido Complex with NHC Ligation: Synthesis, Structure, and Reactivity. *Angew. Chem., Int. Ed.* **2015**, *54*, 12640−12644.
(43) Liu, Y.; Du, J.; Deng, L. Synthesis, Structure, and Reactivity of Low-Spin Cobalt(II) Imido Complexes $[(Me_3P)_3Co(NAr)]$. *Inorg. Chem.* **2017**, *56*, 8278−8286.
(44) Cheng, J.; Liu, J.; Leng, X.; Lohmiller, T.; Schnegg, A.; Bill, E.; Ye, S.; Deng, L. A Two-Coordinate Iron(II) Imido Complex with NHC Ligation: Synthesis, Characterization, and Its Diversified Reactivity of Nitrene Transfer and C-H Bond Activation. *Inorg. Chem.* **2019**, *58*, 7634−7644.
(45) Martinez, J. L.; Lutz, S. A.; Yang, H.; Xie, J.; Telser, J.; Hoffman, B. M.; Carta, V.; Pink, M.; Losovyj, Y.; Smith, J. M. Structural and Spectroscopic Characterization of an Fe(VI) Bis(imido) Complex. *Science* **2020**, *370*, 356−359.
(46) Kumar, A.; Blakemore, J. D. On the Use of Aqueous Metal-Aqua pK_a Values as a Descriptor of Lewis Acidity. *Inorg. Chem.* **2021**, *60*, 1107−1115.
(47) Fukuzumi, S.; Ohkubo, K. Metal Ion-Coupled and Decoupled Electron Transfer. *Coord. Chem. Rev.* **2010**, *254*, 372−385.
(48) Fukuzumi, S.; Ohkubo, K.; Lee, Y. M.; Nam, W. Lewis Acid Coupled Electron Transfer of Metal-Oxygen Intermediates. *Chem.—Eur. J.* **2015**, *21*, 17548−17559.
(49) Fukuzumi, S.; Morimoto, Y.; Kotani, H.; Naumov, P.; Lee, Y. M.; Nam, W. Crystal Structure of a Metal Ion-Bound Oxoiron(IV) Complex and Implications for Biological Electron Transfer. *Nat. Chem.* **2010**, *2*, 756−759.
(50) Morimoto, Y.; Kotani, H.; Park, J.; Lee, Y. M.; Nam, W.; Fukuzumi, S. Metal Ion-Coupled Electron Transfer of a Nonheme Oxoiron(IV) Complex: Remarkable Enhancement of Electron-Transfer Rates by Sc^{3+}. *J. Am. Chem. Soc.* **2011**, *133*, 403−405.
(51) Park, J.; Morimoto, Y.; Lee, Y. M.; Nam, W.; Fukuzumi, S. Metal Ion Effect on the Switch of Mechanism from Direct Oxygen Transfer to Metal Ion-Coupled Electron Transfer in the Sulfoxidation of Thioanisoles by a Non-Heme Iron(IV)-Oxo Complex. *J. Am. Chem. Soc.* **2011**, *133*, 5236−5239.
(52) Kundu, S.; Miceli, E.; Farquhar, E.; Pfaff, F. F.; Kuhlmann, U.; Hildebrandt, P.; Braun, B.; Greco, C.; Ray, K. Lewis Acid Trapping of an Elusive Copper-Tosylnitrene Intermediate Using Scandium Triflate. *J. Am. Chem. Soc.* **2012**, *134*, 14710−14713.
(53) Wang, Q.; Guo, J.; Chen, P. The Impact of Alkali and Alkaline Earth Metals on Green Ammonia Synthesis. *Chem.* **2021**, *7*, 3203−3220.
(54) Ong, T.-G.; Yap, G. P. A.; Richeson, D. S. Catalytic Construction and Reconstruction of Guanidines: Ti-Mediated Guanylation of Amines and Transamination of Guanidines. *J. Am. Chem. Soc.* **2003**, *125*, 8100−8101.

https://doi.org/10.1021/acs.accounts.3c00511
Acc. Chem. Res. 2023, 56, 3392−3403

(55) Lutz, S. A.; Hickey, A. K.; Gao, Y.; Chen, C. H.; Smith, J. M. Two-State Reactivity in Iron-Catalyzed Alkene Isomerization Confers σ-Base Resistance. *J. Am. Chem. Soc.* **2020**, *142*, 15527−15535.
(56) Klein, J.; Becker, J. Y. Metalation Reactions-XIV. The Generality of the 1,3-Sigmatropic Shift of Hydrogen in Allenyllithium Compounds. *Tetrahedron* **1972**, *28*, 5385−5392.
(57) Stephenson, L. M.; Mattern, D. L. Stereochemistry of an Ene Reaction of Dimethyl Azodicarboxylate. *J. Org. Chem.* **1976**, *41*, 3614−3619.
(58) Fernandez, S.; Gonzalez, J.; Santamaria, J.; Ballesteros, A. Propargylsilanes as Reagents for Synergistic Gold(I)-Catalyzed Propargylation of Carbonyl Compounds: Isolation and Characterization of σ-Gold(I) Allenyl Intermediates. *Angew. Chem., Int. Ed.* **2019**, *58*, 10703−10707.
(59) Wang, Y.; Zhu, J.; Durham, A. C.; Lindberg, H.; Wang, Y. M. α-C-H Functionalization of π-Bonds Using Iron Complexes: Catalytic Hydroxyalkylation of Alkynes and Alkenes. *J. Am. Chem. Soc.* **2019**, *141*, 19594−19599.
(60) Cram, D. J.; Uyeda, R. T. Electrophilic Substitution at Saturated Carbon. XXII. Intramolecular Hydrogen Transfer Reactions in Base-Catalyzed Allylic Rearrangements. *J. Am. Chem. Soc.* **1964**, *86*, 5466−5477.
(61) Ela, S. W.; Cram, D. J. Electrophilic Substitution at Saturated Carbon. XXX. Behavior of Phenylallylic Anions and Their Conjugate Acids. *J. Am. Chem. Soc.* **1966**, *88*, 5791−5802.
(62) Bowden, K.; Cook, S. R. Reactions in Strongly Basic Solutions. Part Vl. Correlation of the Rates of Rearrangement of Weak Carbon Acids in Aqueous Dimethyl Sulfoxide with an Acidity Function. Substituent and Kinetic Isotope Effects. *J. Chem. Soc., Perkin Trans.* **1972**, *2*, 1407−1411.
(63) Hassam, M.; Taher, A.; Arnott, G. E.; Green, I. R.; van Otterlo, W. A. Isomerization of Allylbenzenes. *Chem. Rev.* **2015**, *115*, 5462−5569.

https://doi.org/10.1021/acs.accounts.3c00511
Acc. Chem. Res. 2023, 56, 3392−3403